

Resonance Spacer Cation-based Heterostructure Enables Efficient and Stable Perovskite Solar Cells

Zijian Deng ^a, Xichuan Yang ^{a,*}, Qingning Hou ^a, Miao Jiang ^a, Huhu Liang ^a, Shukang Li ^a, Mengde Zhai ^b, Haoxin Wang ^b, Ming Cheng ^{b,*}, Li Zhang ^c, and Licheng Sun ^d

^a Institute of Artificial Photosynthesis, State Key Laboratory of Fine Chemicals, Dalian University of Technology (DUT), 116024 Dalian, China.

^b Institute for Energy Research, Jiangsu University, Zhenjiang 212013, China.

^c Nanjing University of Posts and Telecommunications, 210003, China.

^d Center of Artificial Photosynthesis for Solar Fuels, School of Science, Westlake University, Hangzhou 310024, China.

* E-mail: yangxc@dlut.edu.cn (Xichuan Yang)

mingcheng@ujs.edu.cn (Ming Cheng)

Experimental section

General Information

SEM was performed with FEI (field Emission Instruments: Nova Nano SEM 450), USA. The UV-vis spectroscopy measurements were recorded with an Agilent 8453 spectrophotometer. The *J-V* characteristics of the solar cells were recorded by a Keithley 2400 source measure unit under the AM 1.5G (100 mW cm⁻²) simulated sunlight, Oriel Sol3A solar simulator (Newport USA, Model: 94023A). Before measurement, the light intensity was calibrated with a Newport calibrated standard Si reference cell (SER. No: 506/0358). A metal mask (0.1 cm²) was applied when being recorded. The *J-V* curves were obtained (1.3 V to -0.1 V) at the scan rate of 50 mV s⁻¹. The incident photo-to-current conversion efficiency (IPCE) measurements were obtained by a Hypermono-light (SM-25, Jasco Co. Ltd./ Japan). Prior to measurement, a standard silicon solar cell was used as reference. UPS was measured with a negative bias voltage (-10 V) applied to the samples using the He(I) (21.22 eV) line in order to shift the spectra from the spectrometer threshold. TPV, IMPS, IMVS, EIS, and dark-CELIV measurements were performed on the Paios, Fluxim AG. TPV curves were measured at 100% offset Intensity, with a pulse length of 15 s, and a follow-up time of 5 s. IMPS and IMVS curves were measured at 90% offset intensity, with an amplitude of 10% offset intensity, the frequency from 1 MHz to 10 Hz. The scan range of EIS

was from 10 MHz to 1 Hz. The dark-CELIV with a sweep ramp rate of 10 V/ms, and the maximum voltage was 3 V. The PL was recorded by FluoroMax-4P (Horiba Jobin Yvon). ^1H and ^{13}C NMR spectroscopy measurements were recorded on a Bruker Avance II 400 spectrometer. In ^1H NMR spectroscopy measurements, the concentrations of AT, AMTI, ABT, and AMBTI are all 0.04 M in DMSO- d_6 , and all spectra were calibrated using the DMSO- d_6 peak at 2.5 ppm. In ^{13}C NMR spectroscopy measurements, all spectra were calibrated using the DMSO- d_6 peak at 39.6 ppm. High-resolution mass spectrometry was performed on the Agilent 6230B instrument.

TRPL (FLS1000 Edinburgh Instruments), XRD (D8 Advance, Bruker corporation), and c-AFM (JPK Nanowizard 4XP, Bruker, Germany) data were obtained using equipment maintained by Instrumental Analysis Center, Dalian University of Technology.

DFT Calculation

ESP:

We ran density functional theory (DFT) B3LYP/6-311+G calculations for the determination of the electrostatic surface potential of AMT^+ and AMBT^+ .

2D mode:

We have employed the Vienna Ab initio Simulation Package (VASP) to perform all density functional theory (DFT) calculations within spin-polarized frame. The elemental core and valence electrons were represented by the projector augmented wave (PAW) method and plane-wave basis functions with a cutoff energy of 450 eV. Generalized gradient approximation with the Perdew-Burke-Ernzerhof (GGA-PBE) exchange-correlation functional was employed in all the calculations. Geometry optimizations were performed with the force convergency smaller than 0.05 eV/Å. The DFT-D3 empirical correction method was employed to describe van der Waals interactions. Monkhorst-Pack k-points of $3 \times 3 \times 1$ were applied for all the calculations. Atoms at bottom are fixed in all the calculation.

Materials

Dimethylformamide (DMF), dimethyl sulfoxide (DMSO), chlorobenzene (CB), 2-Aminothiazole, and 2-Benzothiazolamine were purchased from Energy chemical (98.0%). Poly(acrylic acid) (paa, M.W ~ 450000) was purchased from Macklin. Tin (IV) oxide colloid dispersion (15 wt%), formamidine iodide (FAI), lead iodide (PbI₂), and Cesium iodide (CsI) were purchased from Advanced Election Technology Co., Ltd. FK 209 Co(III), 4-tertbutylpyridine (t-BuPy), and lithium bis(trifluoromethanesulfonyl)imide (Li-TFSI) were purchased from Xi'an Polymer Light Technology in China. Spiro-OMeTAD was purchased from Dalian HeptaChroma SolarTech Co., Ltd. All chemicals were used without further purification.

Solution preparation

The paa-QD-SnO₂ precursor solution contains 4 ml of Tin (IV) oxide colloid dispersion (15 wt%), 100 ml of water and 40 mg of Poly (acrylic acid) (paa, M.W ~ 450000).¹

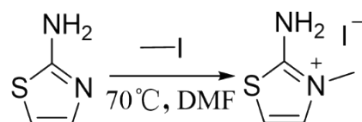
FA_{0.88}Cs_{0.12}PbI₃ perovskite precursor solutions (1.25 M) were prepared by directly dissolving 495.6 mg PbI₂, 151.4 mg FAI, 31.2 mg CsI, 13 mg MAcl into 0.8 mL anhydrous DMF:DMSO with a volume ratio of 8:1. The Spiro-OMeTAD solution was prepared by mixing 73.5 mg Spiro-OMeTAD, 17.5 μL Li-TFSI solution (520 mg Li-TFSI in 1 mL acetonitrile), 28.8 μL tBP, and 29 μL FK 209 Co(III) solution (300 mg in 1 mL acetonitrile) in 1 mL chlorobenzene.

Perovskite solar cell fabrication

Pre-patterned FTO was cleaned in soapy water, deionized water, acetone and ethanol with sonication and then all substrates were UV-ozone cleaned for 30 min subsequently before further use, and then deposited with a thin compact TiO₂ layer by spray pyrolysis using 0.2 M Ti(acac)₂OiPr₂ in EtOH solution at 500 °C. The sprayed film was annealed at 500 °C for 30 min. And tin oxide was utilized as electron transport material. And the solution was spun onto the glass/compact TiO₂ substrate surface at 4000 rpm for 30 s, and then baked on a hotplate in ambient atmosphere at 160 °C for 30 min. Then

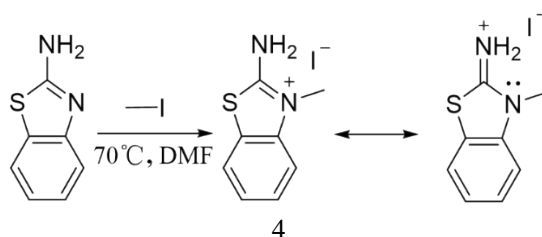
substrates were UV-ozone cleaned for 30 min subsequently before depositing perovskite. The perovskite solution was spin-coated in a two-step program at 1000 and 5000 rpm for 10 and 30 s, respectively. During the second step, 150 μL of chlorobenzene was poured on the spinning substrate 15 s prior to the end of the program. The wet film was annealed at 100°C for 60 min. For the AMTI or AMBTI-modified samples, the IPA solution of 2 mg/ml AMTI or 2 mg/ml AMBTI was coated on the cooled substrate at 1500 rpm for 30 s by dynamic spin-coating, then annealed at 100 °C for 5 min, repeated several times (The rationale behind adopting this approach is rooted in the fact that both substances have a limited solubility in IPA), the number of modifications for 1D/3D and 2D/3D is once and twice, respectively (see **Fig. S11** and **Tab. S4**), in all of tests. After the perovskite cooled down to room temperature, the spiro-OMeTAD was spin-coated at 3000 rpm for 30 s. Finally, 100 nm of the silver top electrode was thermally evaporated under 7×10^{-4} Pa vacuum. All the procedures were completed in ambient environment with relative humidity below 25%.

Synthetic procedures



2-amino-3-methylthiazol-3-ium iodide (AMTI):

2.0 g 2-Aminothiazole and 2 ml CH_3I were dissolved in 30 ml DMF and kept stirring for 4 hours at 70 °C. After cooling to room temperature, the crude product was separated out with CH_2Cl_2 . And then further purified by recrystallization (1.31 g, 65%), with methanol and ether as the benign solvent and the poor solvent, respectively. ^1H NMR (400 MHz, DMSO- d_6) δ 9.32 (s, 2H), 7.40 (d, $J = 4.5$ Hz, 1H), 7.00 (d, $J = 4.5$ Hz, 1H), 3.58 (s, 3H). ^{13}C NMR (400 MHz, DMSO- d_6) δ 167.99, 131.13, 107.27, 35.51. Mass spectrum m/z calculated for $\text{C}_4\text{H}_7\text{N}_2\text{S}^+$: 115.0324; found, 115.0328.



2-amino-3-methylbenzo[d]thiazol-3-ium iodide (AMBTI):

3.0 g 2-Benzothiazolamine and 2 ml CH₃I were dissolved in 50 ml DMF and kept stirring for 4 hours at 70 °C. After cooling to room temperature, the crude product was separated out with CH₂Cl₂. And then further purified by recrystallization (1.83 g, 61%), with methanol and ether as the benign solvent and the poor solvent, respectively. ¹H NMR (400 MHz, DMSO-d₆) δ 9.99 (s, 2H), 8.00 (d, *J* = 7.9 Hz, 1H), 7.68 (d, *J* = 8.1 Hz, 1H), 7.58 (td, *J* = 7.6, 1.2 Hz, 1H), 7.43 (td, *J* = 8.0, 0.8 Hz, 1H), 3.73 (s, 3H). ¹³C NMR (400 MHz, DMSO-d₆) δ 168.07, 138.99, 127.79, 125.21, 123.59, 122.26, 111.43, 32.39. Mass spectrum *m/z* calculated for C₈H₉N₂S⁺: 165.0481; found, 165.0424.

AMTPbI₃:

242 mg AMTI and 461 mg PbI₂ were dissolved in 1 ml DMF and kept stirring for 1 hour at 100 °C. After cooling, transfer it into a methanol atmosphere and induce crystallization through solvent diffusion at 65 °C.

AMBTPbI₃·2DMF

146 mg AMBTI and 230.5 mg PbI₂ were dissolved in 2 ml DMF and kept stirring for 1 hour at 100 °C. Crystals AMBTPbI₃·2DMF can be obtained by natural cooling and standing for 2 hours.

(AMBT)₂PbI₄:

73 mg AMBTI and 115.2 mg PbI₂ were dissolved in 5 ml DMF and kept stirring for 1 hour at 60 °C. (AMBT)₂PbI₄ film was obtained by spin-coating on the glass annealed at 150 °C for 10 minutes.

Table S1. Details of X-ray crystallographic parameters of AMTPbI₃.

CCDC Number	CCDC:2310300
Empirical formula	C ₄ H ₇ I ₃ N ₂ PbS
Formula weight	703.07
Temperature/K	99.2(2)
Crystal system	orthorhombic
Space group	Pna2 ₁
a/Å	14.7651(4)
b/Å	9.7520(3)
c/Å	8.6221(3)
α/°	90
β/°	90
γ/°	90
Volume/Å ³	1241.49(7)
Z	4
ρ _{calc} /cm ³	3.762
μ/mm ⁻¹	21.172
F(000)	1208.0
Crystal size/mm ³	0.1 × 0.1 × 0.08
Radiation	Mo Kα (λ = 0.71073)
2θ range for data collection/°	7.266 to 60.682
Index ranges	-20 ≤ h ≤ 20, -12 ≤ k ≤ 13, -12 ≤ l ≤ 11
Reflections collected	15809
Independent reflections	3276 [R _{int} = 0.0391, R _{sigma} = 0.0291]
Data/restraints/parameters	3276/1/101
Goodness-of-fit on F ²	1.092
Final R indexes [I ≥ 2σ (I)]	R ₁ = 0.0195, wR ₂ = 0.0439
Final R indexes [all data]	R ₁ = 0.0203, wR ₂ = 0.0442
Largest diff. peak/hole / e Å ⁻³	1.27/-1.46
Flack parameter	0.418(8)

Table S2. Details of X-ray crystallographic parameters of AMBTPbI₃·2DMF.

CCDC Number	CCDC:2242973
Empirical formula	C ₁₄ H ₂₃ I ₃ N ₄ O ₂ PbS
Formula weight	899.361
Temperature/K	296.15
Crystal system	triclinic
Space group	P-1
a/Å	8.2105(7)
b/Å	12.7412(11)
c/Å	13.2110(12)
α/°	113.912(2)
β/°	102.036(2)
γ/°	93.293(2)
Volume/Å ³	1219.95(19)
Z	2
ρ _{calc} /cm ³	2.448
μ/mm ⁻¹	10.812
F(000)	809
Crystal size/mm ³	0.12 × 0.1 × 0.08
Radiation	Mo Kα (λ = 0.71073)
2θ range for data collection/°	5.14 to 50
Index ranges	-10 ≤ h ≤ 10, -16 ≤ k ≤ 14, -17 ≤ l ≤ 15
Reflections collected	8194
Independent reflections	4168 [R _{int} = 0.0263, R _{sigma} = 0.0444]
Data/restraints/parameters	4168/0/230
Goodness-of-fit on F ²	1.032
Final R indexes [I ≥ 2σ (I)]	R ₁ = 0.0260, wR ₂ = 0.0667
Final R indexes [all data]	R ₁ = 0.0305, wR ₂ = 0.0698
Largest diff. peak/hole / e Å ⁻³	0.92/-0.66

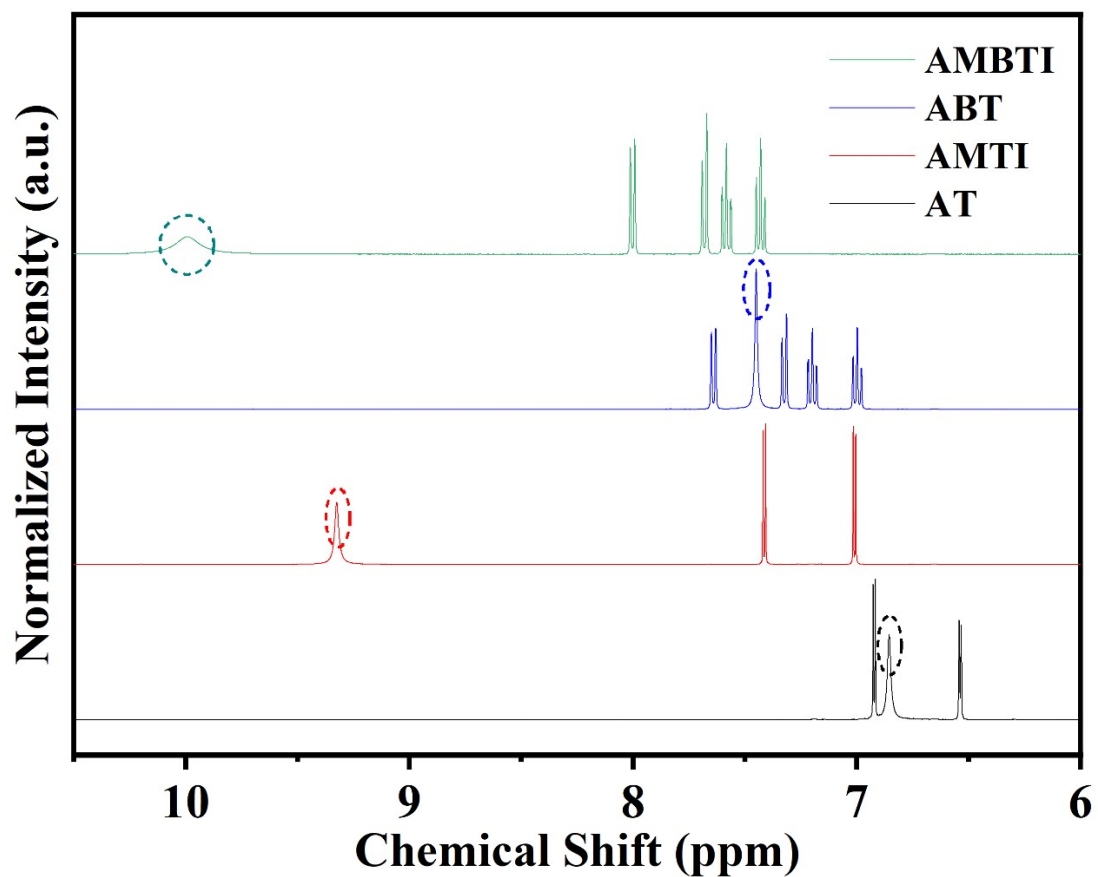


Figure S1a ¹H NMR spectra of AT, AMTI, ABT, and AMBTI in DMSO-d₆ solution at 400 MHz and 25°C. The dashed circles indicate amido. The concentrations of AT, AMTI, ABT, and AMBTI are all 0.04 M, and all spectra were calibrated using the DMSO-d₆ peak at 2.5 ppm.

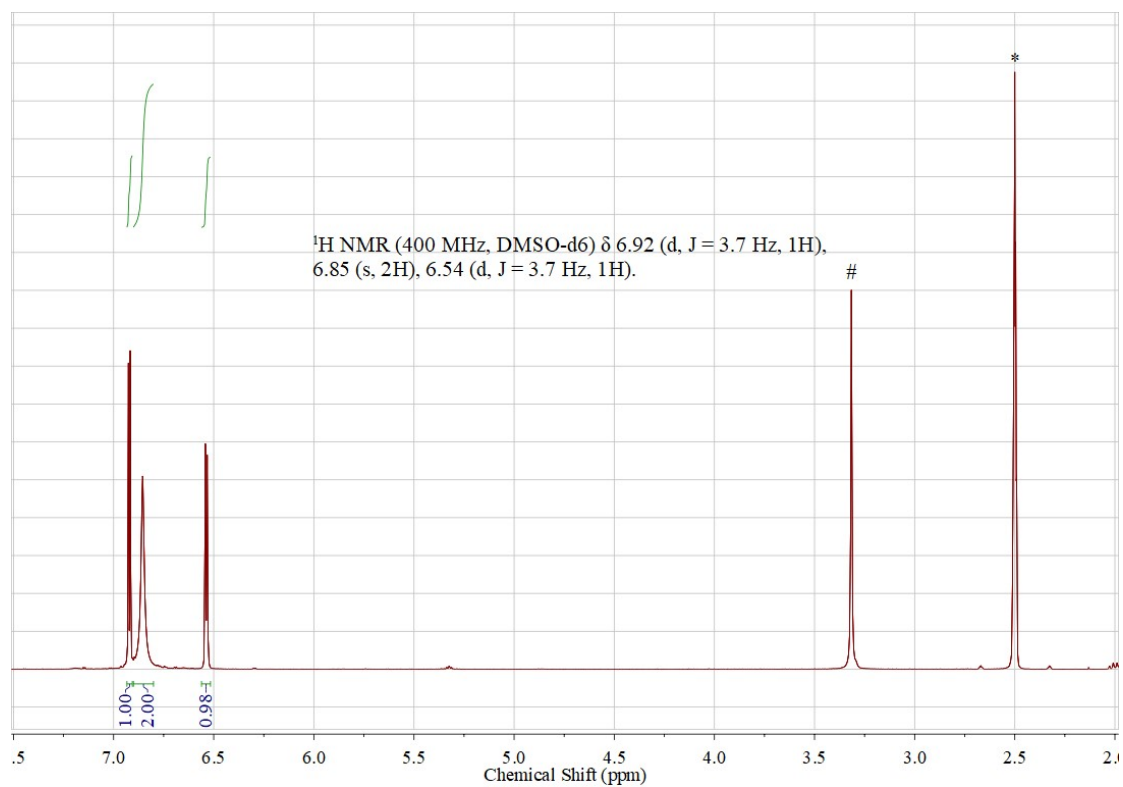


Figure S1b ¹H NMR spectrum of AT in DMSO-d₆ solution at 400 MHz and 25°C.

“#” is the peak of water, and “*” is the peak of DMSO.

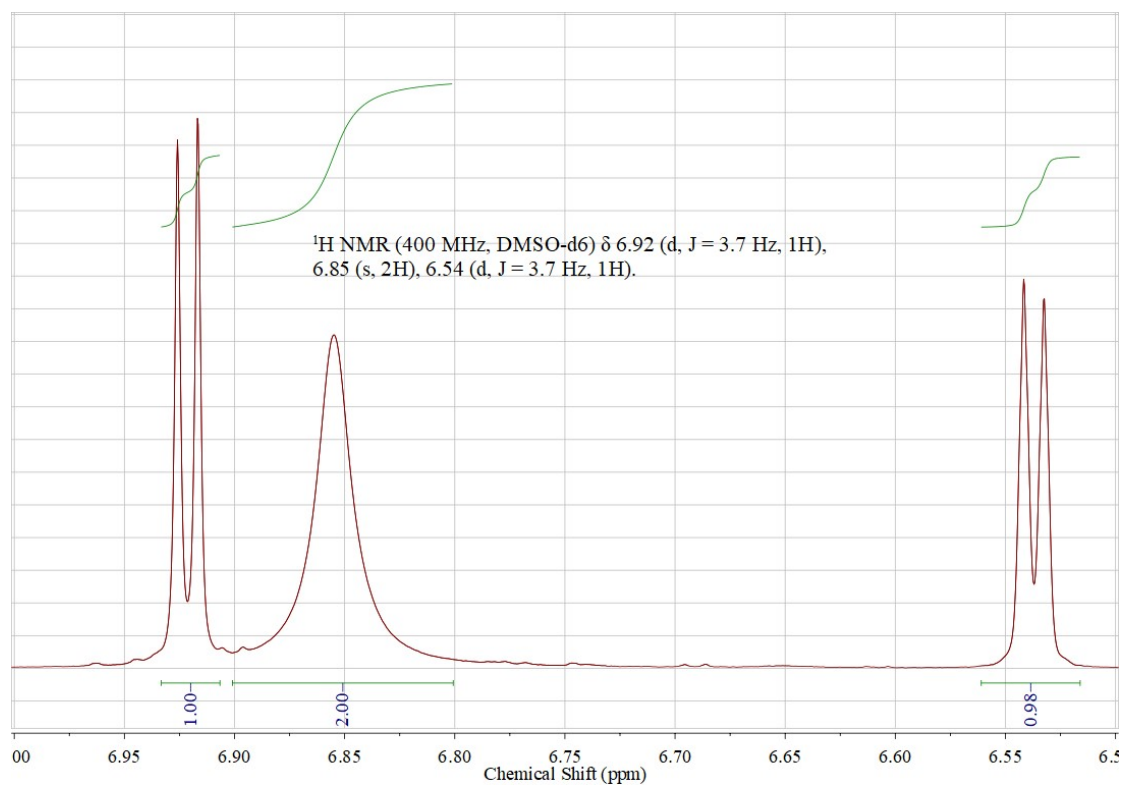


Figure S1c ¹H NMR spectrum of AT in DMSO-d₆ solution at 400 MHz and 25°C (7.0 to 6.5).

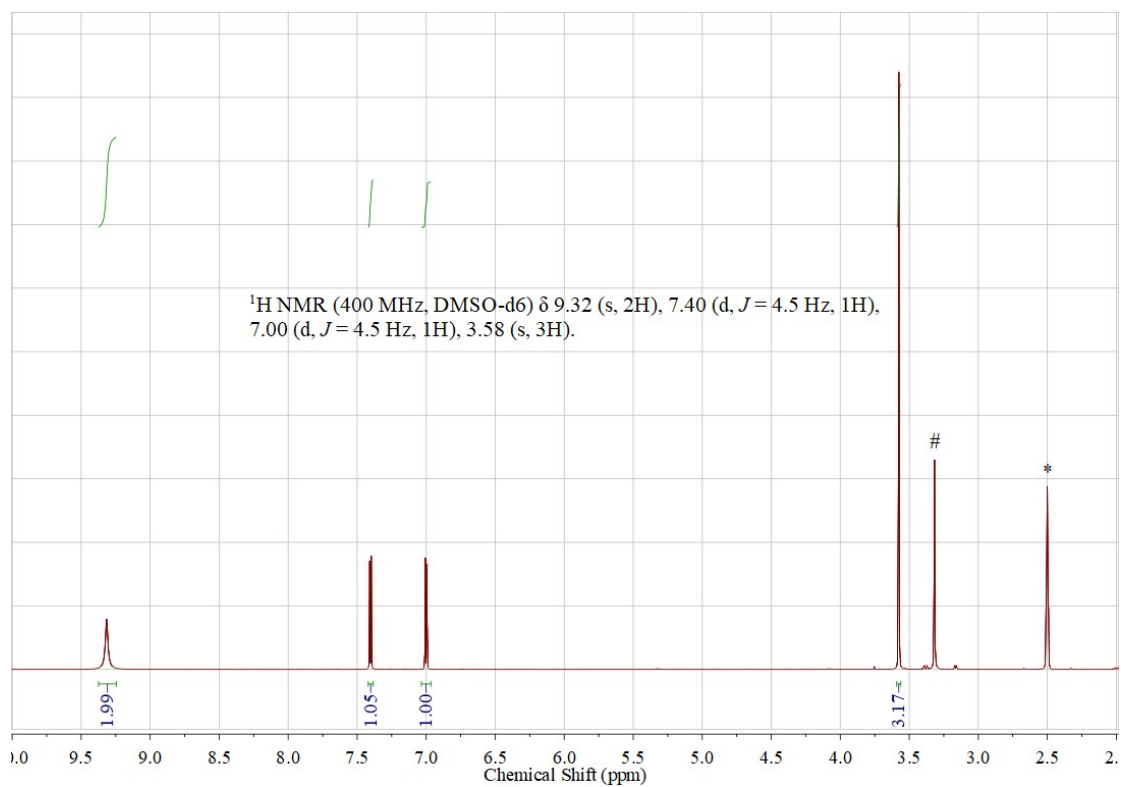


Figure S1d $^1\text{H NMR}$ spectrum of AMTI in DMSO- d_6 solution at 400 MHz and 25°C. “#” is the peak of water, and “*” is the peak of DMSO.

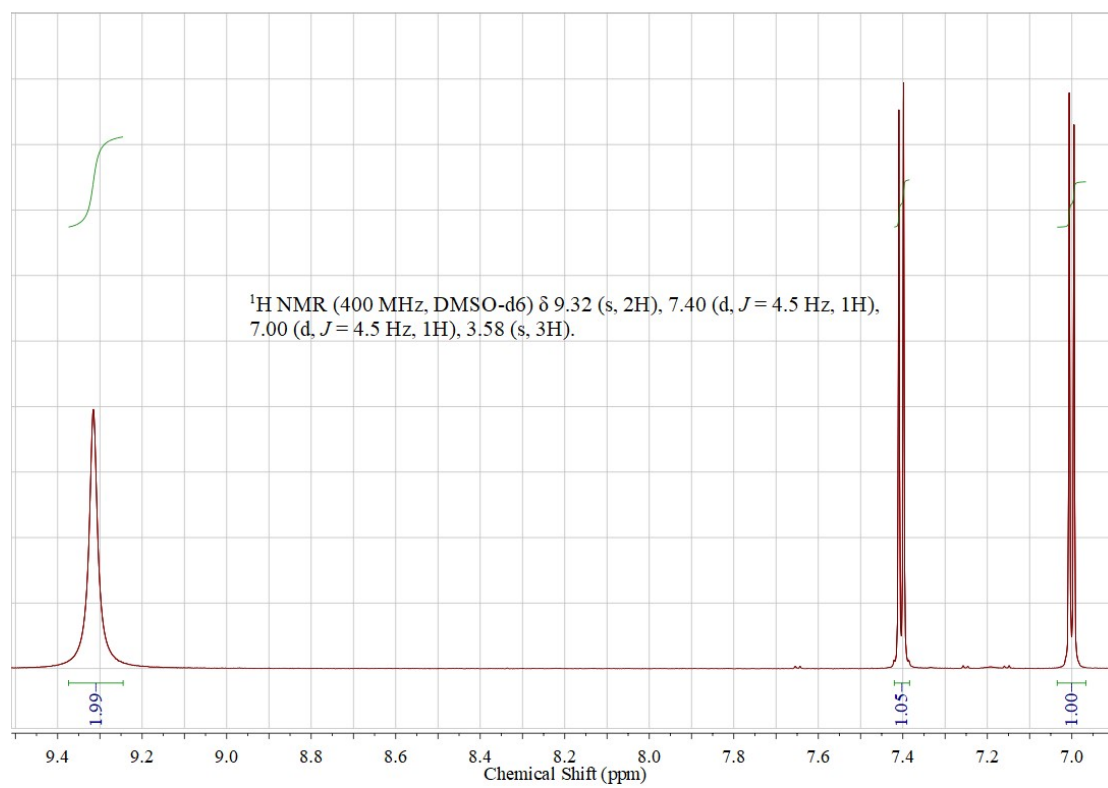


Figure S1e $^1\text{H NMR}$ spectrum of AMTI in DMSO- d_6 solution at 400 MHz and 25°C (9.5 to 6.9).

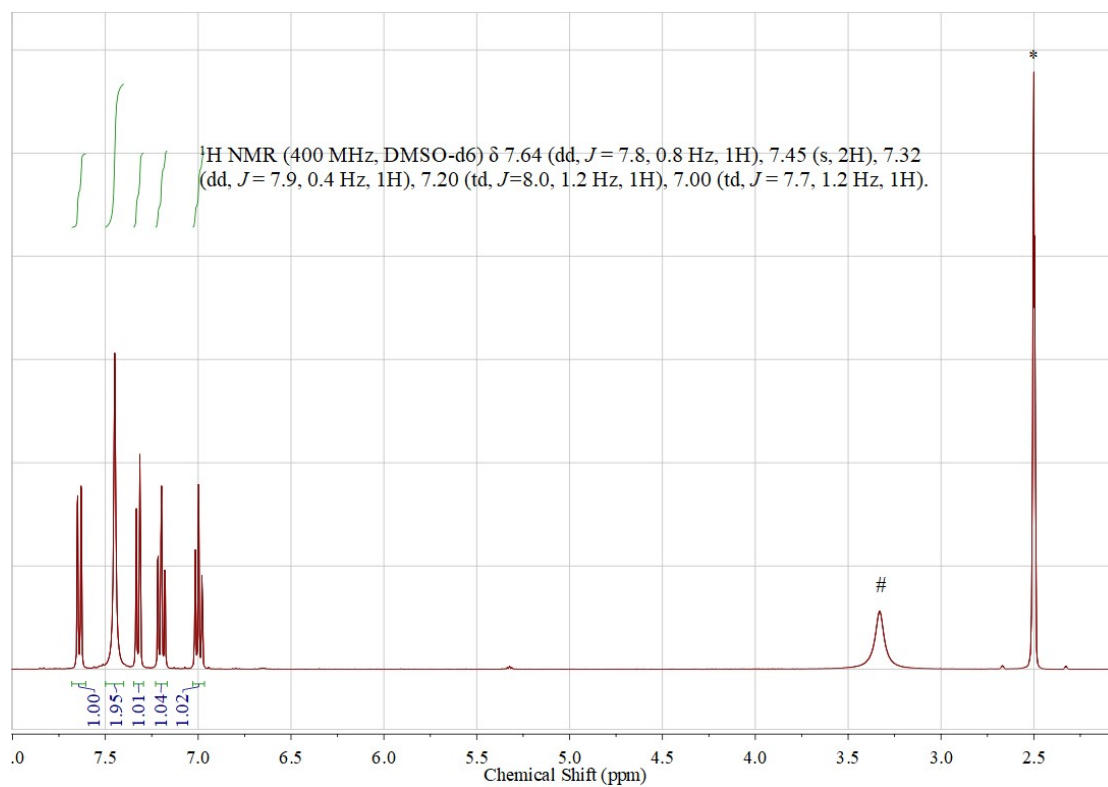


Figure S1f ^1H NMR spectrum of ABT in DMSO- d_6 solution at 400 MHz and 25°C.

“#” is the peak of water, and “*” is the peak of DMSO.

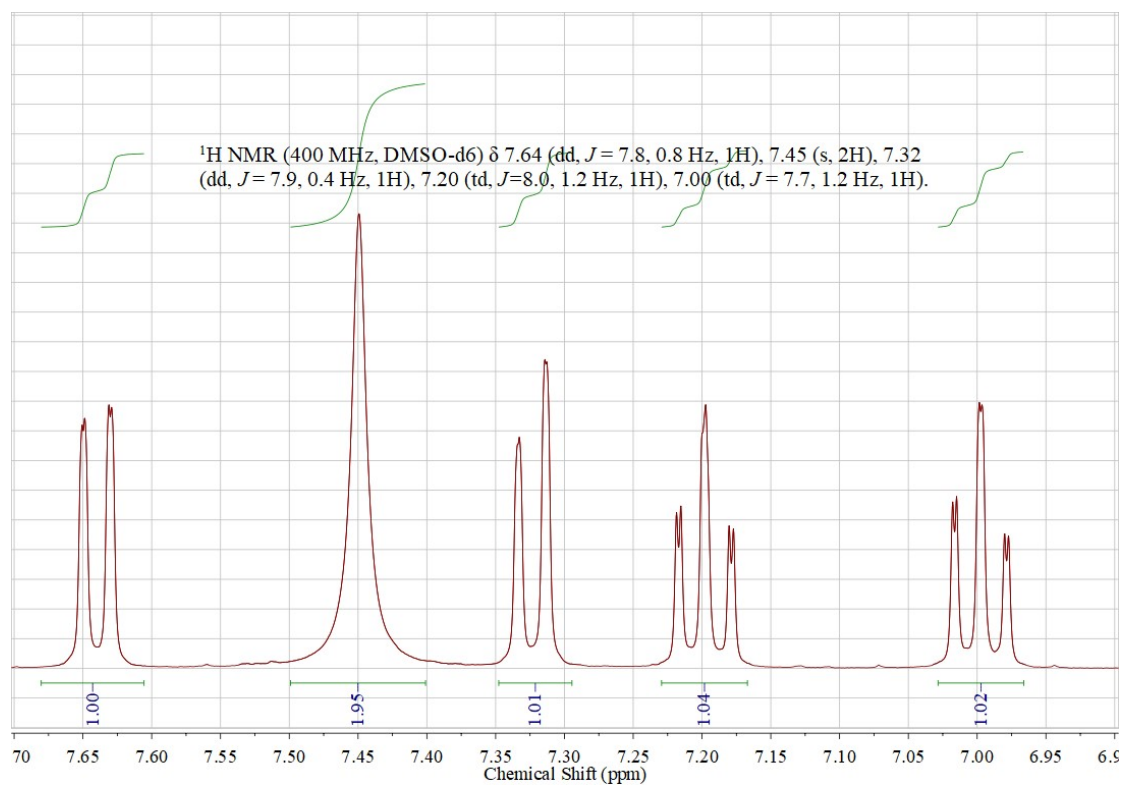


Figure S1g ^1H NMR spectrum of ABT in DMSO- d_6 solution at 400 MHz and 25°C

(7.7 to 6.9).

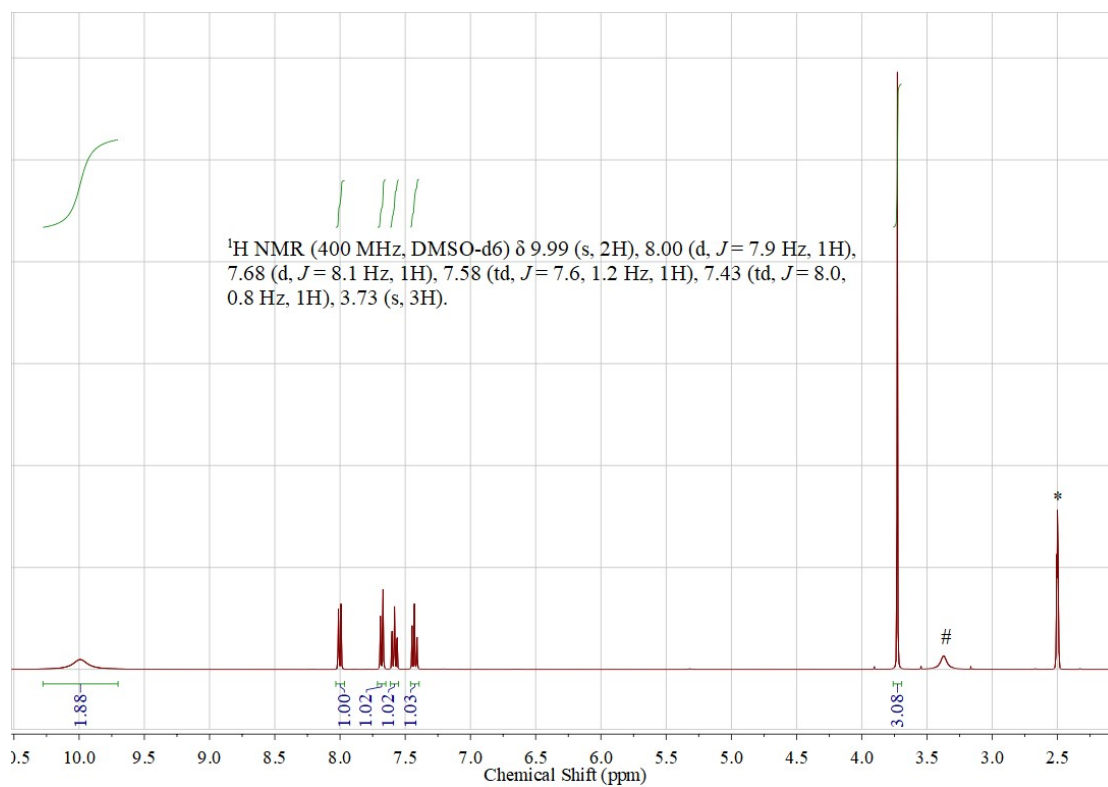


Figure S1h ¹H NMR spectrum of AMBTI in DMSO-d₆ solution at 400 MHz and 25°C. “#” is the peak of water, and “*” is the peak of DMSO.

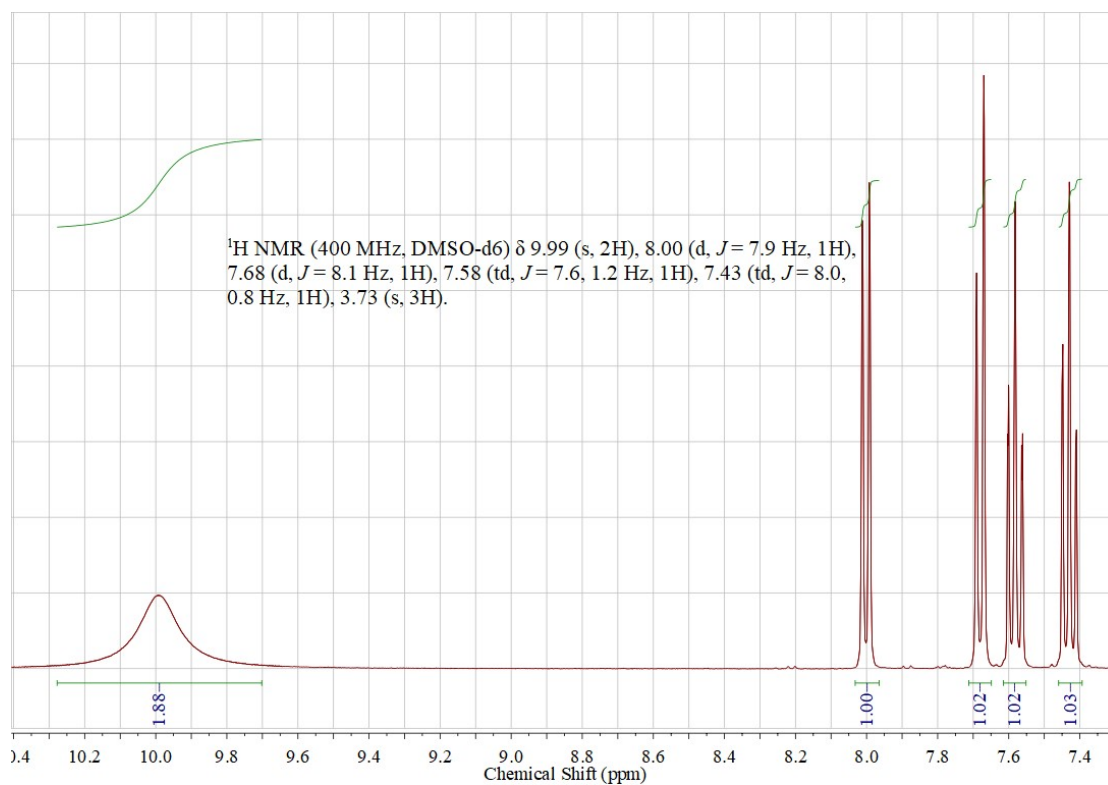


Figure S1i ¹H NMR spectrum of AMBTI in DMSO-d₆ solution at 400 MHz and 25°C (10.4 to 7.3).

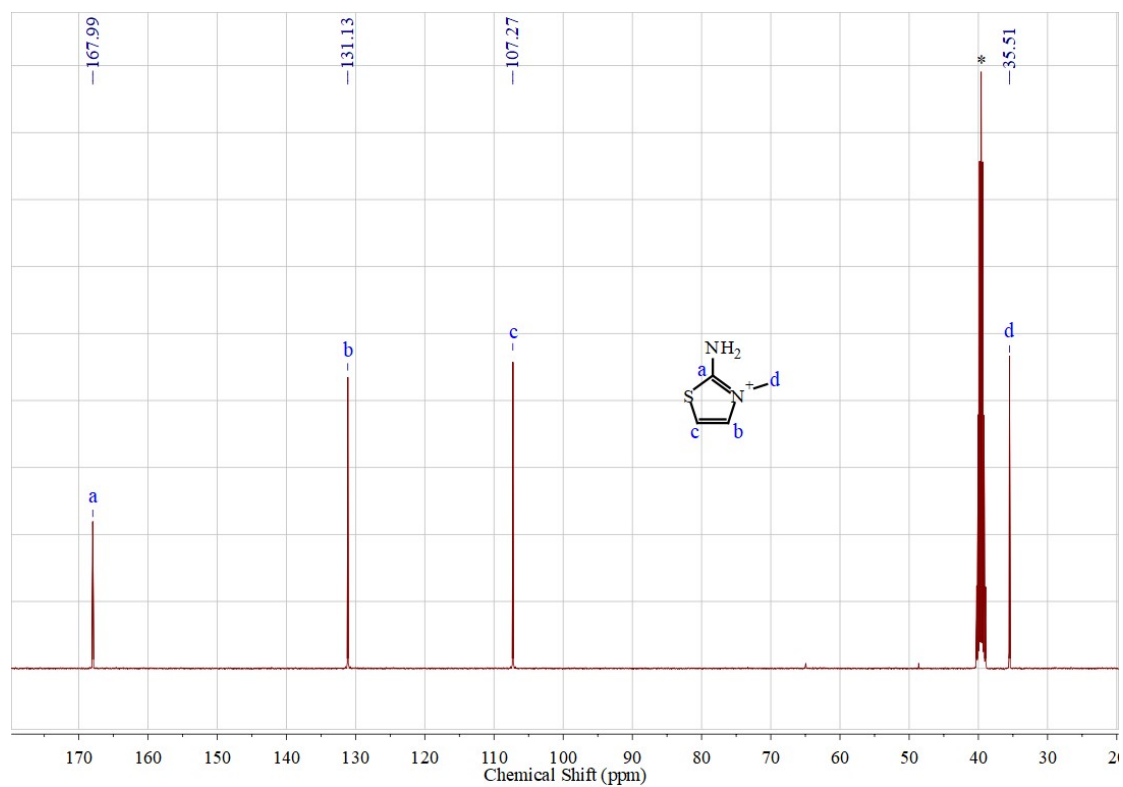


Figure S1j. ^{13}C NMR spectrum of AMTI in DMSO- d_6 solution at 100 MHz and 25°C. “*” is the peak of DMSO- d_6 .

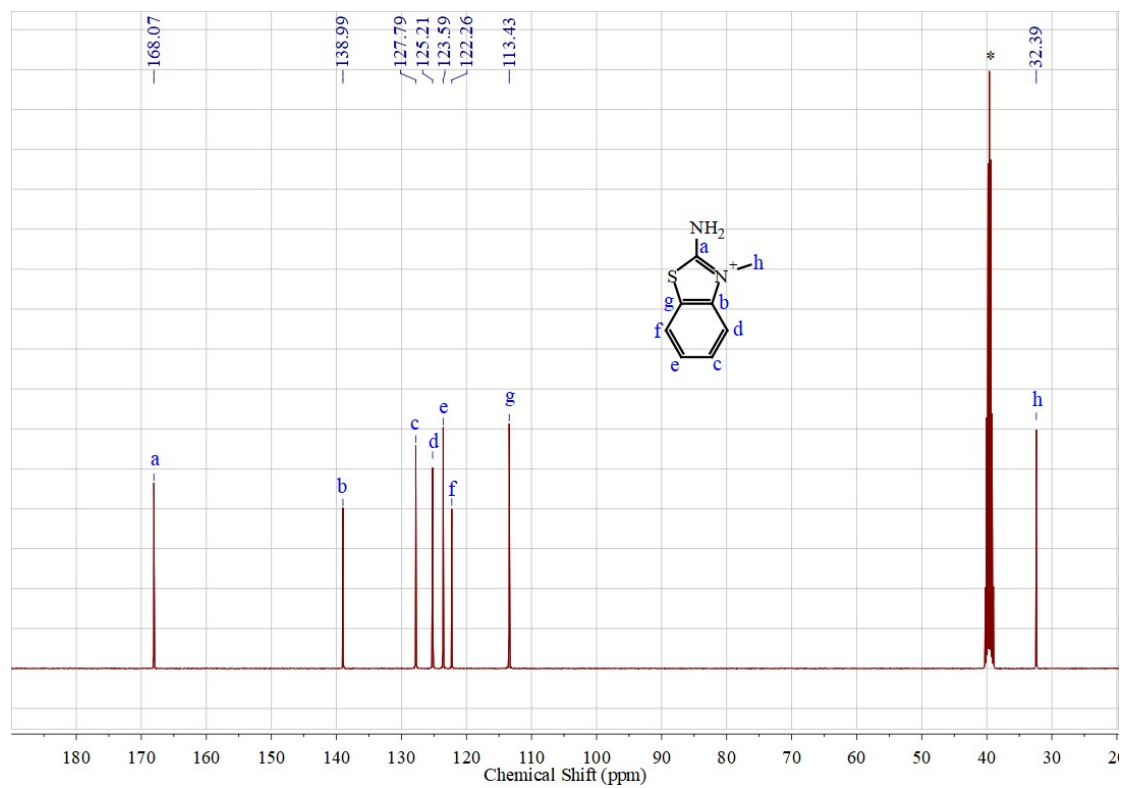


Figure S1k. ^{13}C NMR spectrum of AMBTI in DMSO- d_6 solution at 100 MHz and 25°C. “*” is the peak of DMSO- d_6 .

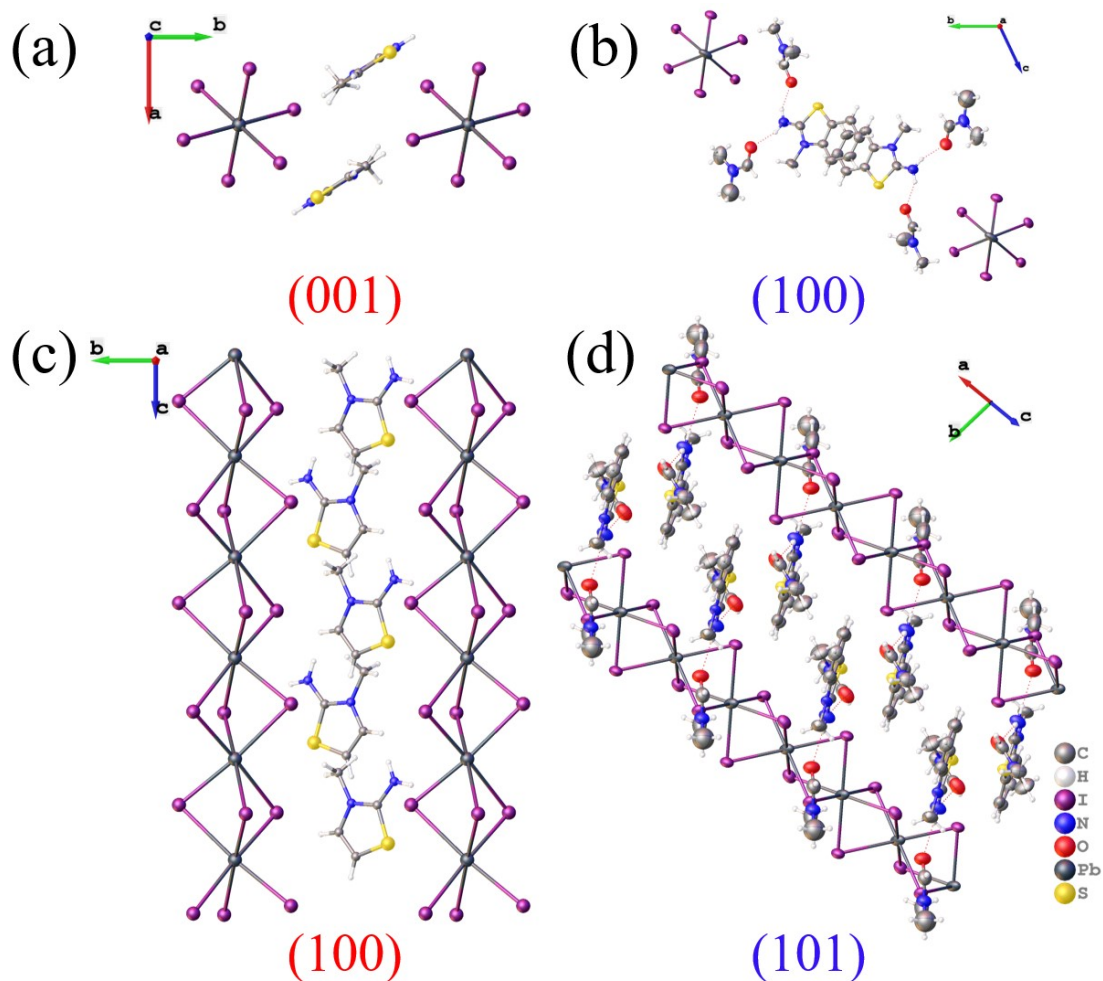


Figure S2. Crystal structures of (a, c) AMTPbI₃ and (b, d) AMBTPbI₃·2DMF under different crystal planes

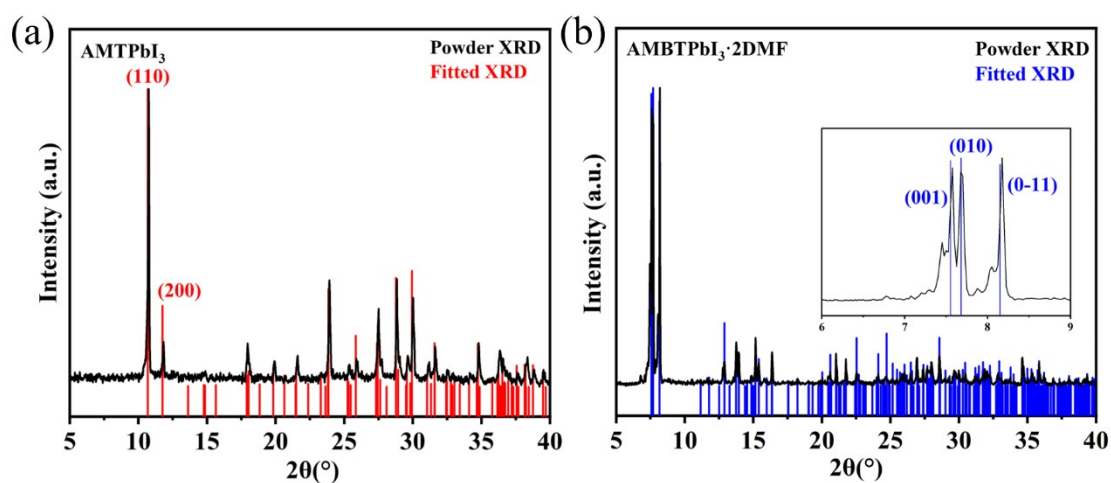


Figure S3. Powder XRD and fitted XRD of (a) AMTPbI₃ and (b) AMBTPbI₃·2DMF

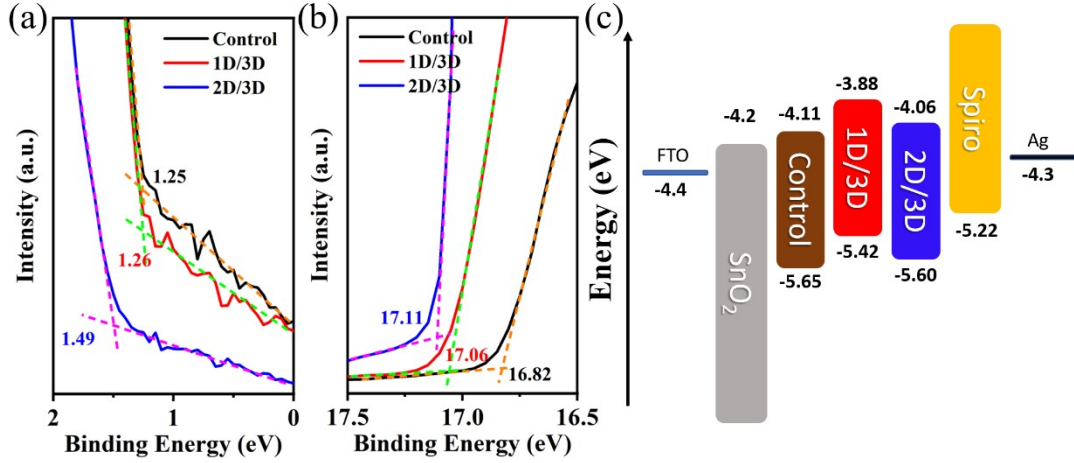


Figure S4. Ultraviolet photoelectron spectra (UPS) (a) start edge (E_{onset}) and (b) cut-off edge (E_{cutoff}) of control, 1D/3D, and 2D/3D films; (c) The energetic levels of all related materials

Equations S1-S3 show the relationship between E_F (Fermi level), E_{VB} , and E_{CB} .

$$E_F = E_{\text{cutoff}} - 21.22 \text{ eV} \quad (\text{S1})$$

$$E_{VB} = E_F - E_{\text{onset}} \quad (\text{S2})$$

$$E_{CB} = E_{VB} + E_g \quad (\text{S3})$$

Table S3. Fitting parameters for the TRPL curves of perovskite films.

	A_1	τ_1/ns	A_2	τ_2/ns	$\tau_{\text{ave}}/\text{ns}$
Control	0.08708	48.11	0.87388	542.80	538.47
1D/3D	0.12867	357.96	0.79985	1129.9	1092.56
2D/3D	0.18652	89.94	0.74865	717.05	698.05

TRPL decay curves were fitted with equation (S4):

$$f(t) = A_1 e^{-\frac{t}{\tau_1}} + A_2 e^{-\frac{t}{\tau_2}} + B \quad (\text{S4})$$

The average PL decay lifetime can be obtained using equation (S5):

$$\tau_{ave} = \frac{\sum_i^A \tau_i^2}{\sum_i^A \tau_i} \quad (S5)$$

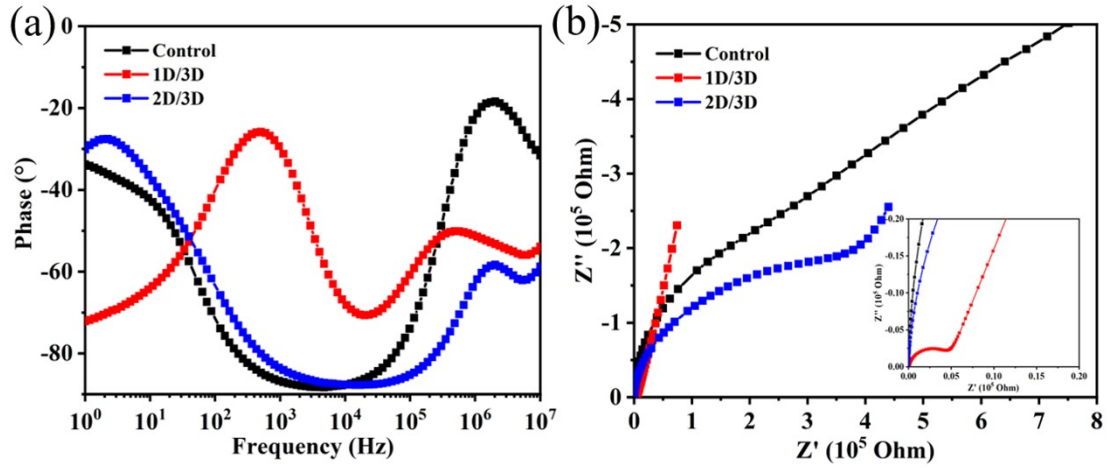
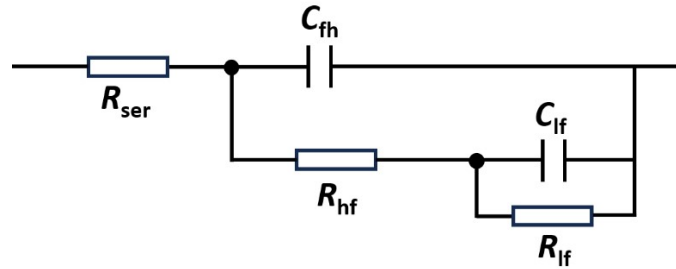


Figure S5. (a) Bode and (b) Nyquist plot of control, 1D/3D, and 2D/3D devices in dark state. The control device has minimum recombination impedance.



Schematic S1. Equivalent circuit of PSCs.

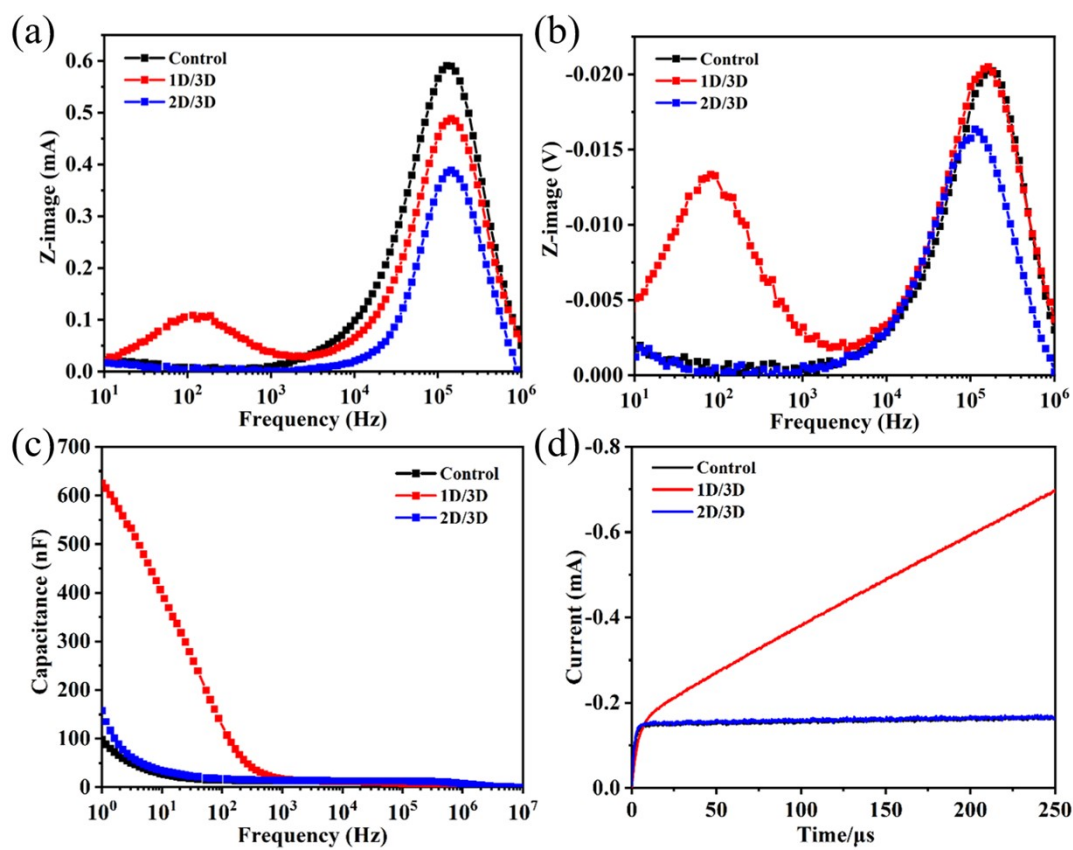


Figure S6. The spectrum of three kinds of devices of (a) IMPS, (b) IMVS, and (c) EIS (capacitance to frequency). (d) Dark-CELIV curves of three types of devices under the extraction voltage slope of 10 V/ms.

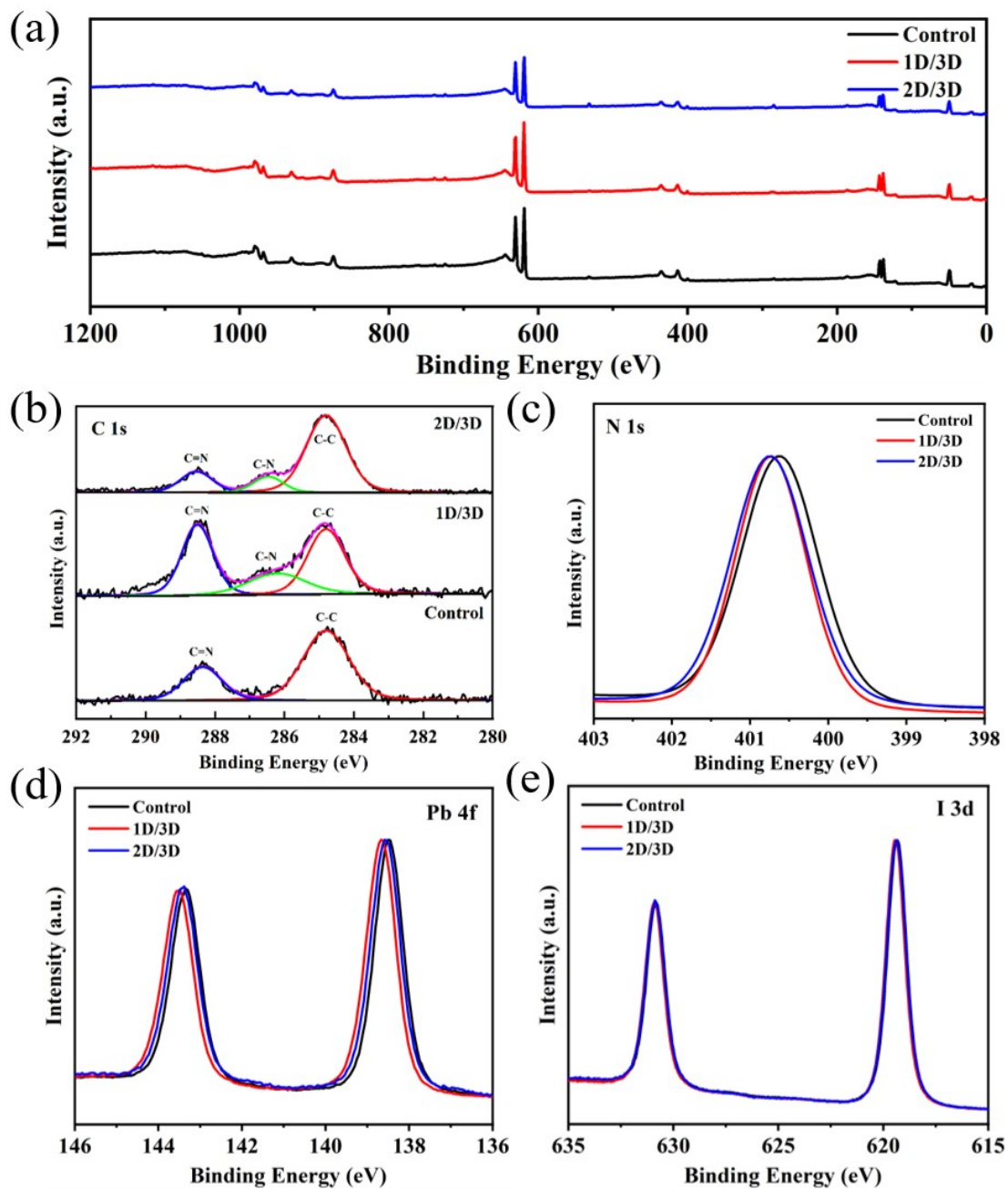


Figure S7. XPS spectra of (a) survey, (b) C 1s, (c) N 1s, (d) Pb 4f, and (e) I 3d.

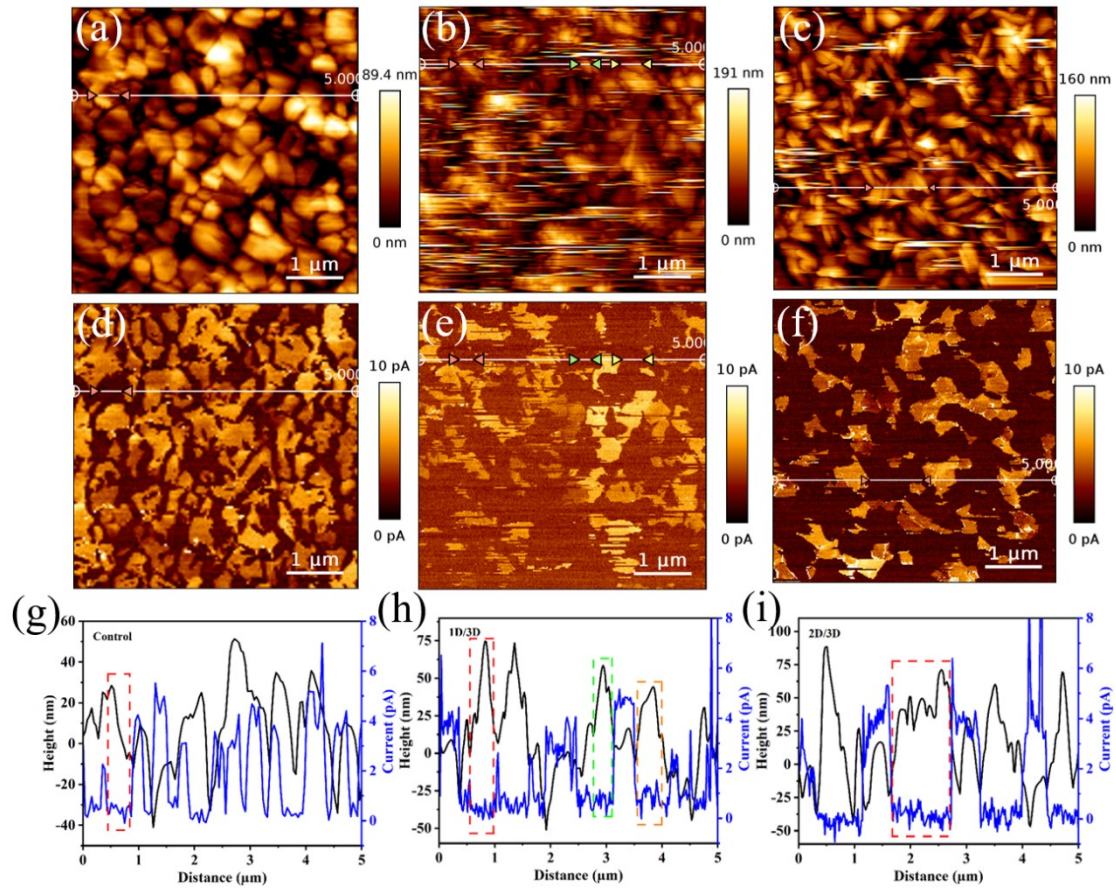


Figure S8. C-AFM topography, current mapping, and corresponding height and current curves along the white line based on (a, d, g) Control, (b, e, h) 1D/3D, and (c, f, i) 2D/3D. The area between the triangles corresponds to the dashed box, and the sample structure is FTO/SnO₂/PVK.

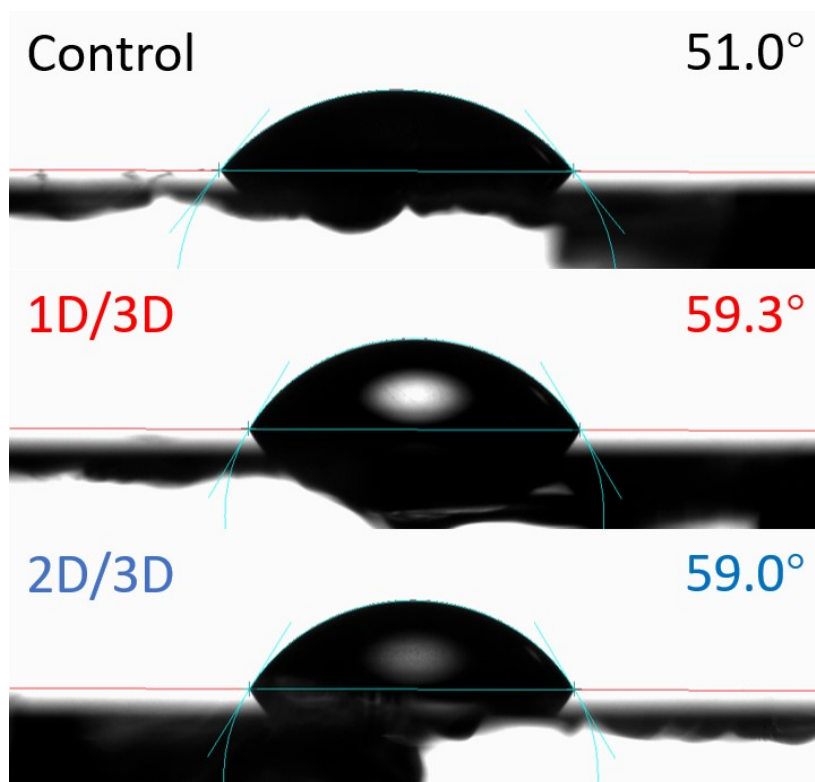


Figure S9. The water contact angle of PVK films of control, 1D/3D, and 2D/3D.

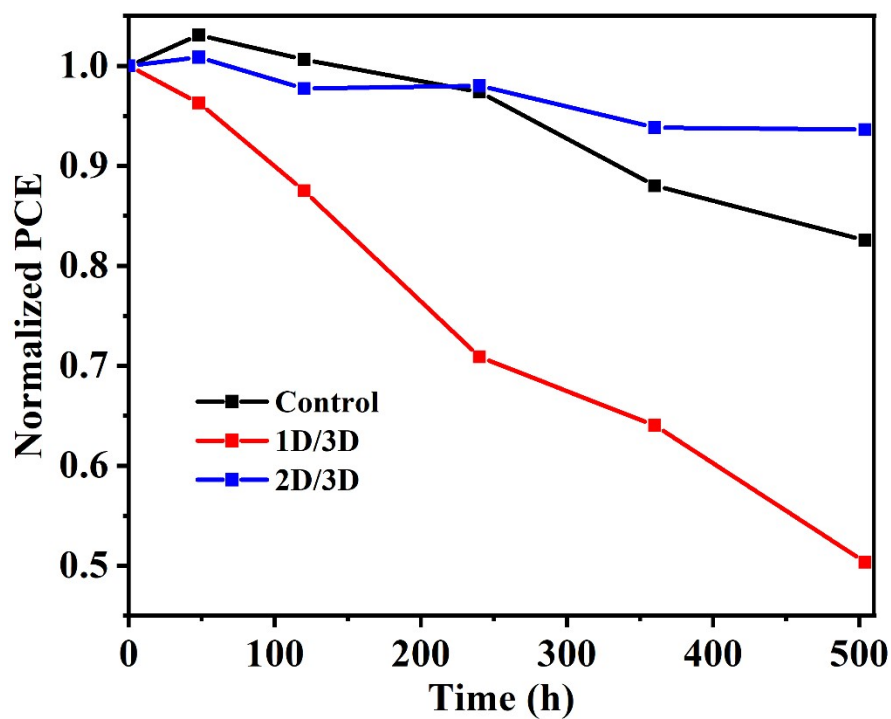


Figure S10. The long-term stability of three types of PSCs at 40% humidity.

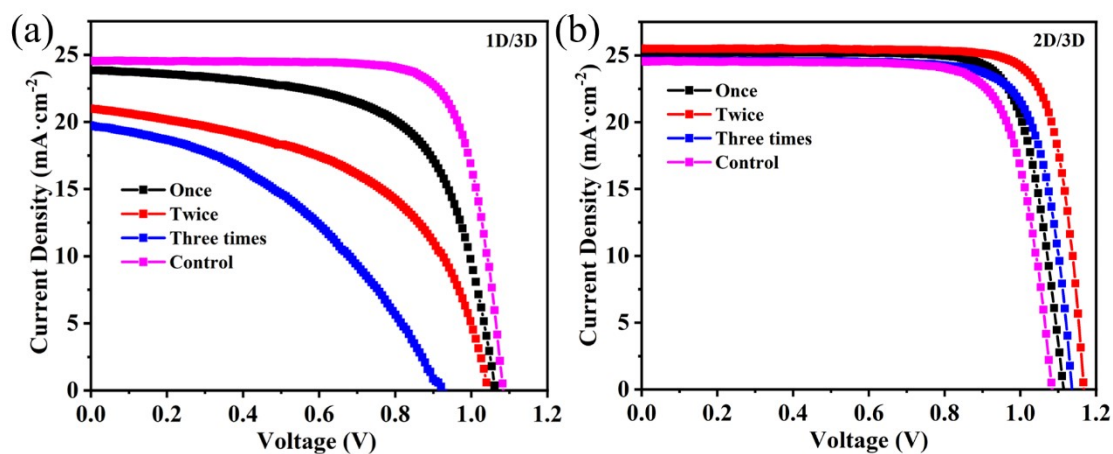


Figure S11. The J - V performance of 1D/3D and 2D/3D PSCs with different number of modifications.

Table S4. The J - V performance of 1D/3D and 2D/3D PSCs with different number of modifications.

Number of modifications		V_{oc} (V)	J_{sc} (mA·cm ⁻²)	FF (%)	PCE (%)
Control	/	1.083	24.56	77.17	20.52
	Once	1.062	23.86	63.76	16.15
1D/3D	Twice	1.042	20.99	52.32	11.45
	Three times	0.921	19.69	41.28	7.49
	Once	1.114	25.23	78.75	22.14
2D/3D	Twice	1.166	25.50	81.36	24.20
	Three times	1.135	24.63	78.38	21.92

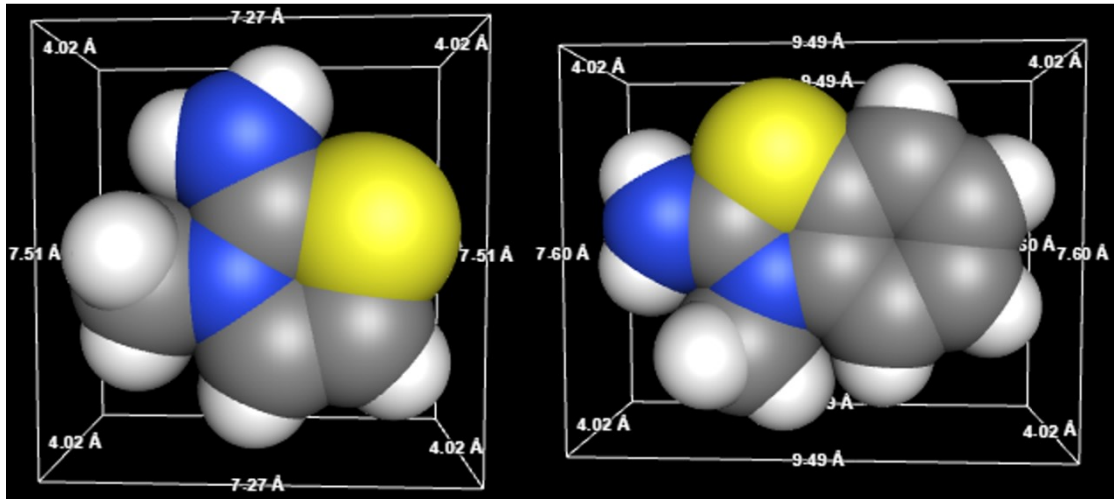


Figure S12. Ion size parameters of AMT⁺ and AMBT⁺.

Table S5. Ion size parameters and corresponding tolerance factor of AMT⁺ and AMBT⁺

Ion	Size	Arithmetic mean	Geometric mean	Tolerance factor
		radius	radius	
AMT ⁺	7.267×7.506×4.018	3.132	3.015	1.09
AMBT ⁺	9.485×7.603×4.019	3.518	3.309	1.15

Table S6. The *J-V* performance of AMBTI/3D PSCs with different rotation speed.

	rotation speed	V_{oc} (V)	J_{sc} (mA·cm ⁻²)	FF (%)	PCE (%)
Control	/	1.077±0.024	24.82±0.45	73.6±3.0	19.7±0.9
With 2 mg/mL	2000	1.072±0.016	24.78±0.30	73.0±3.0	19.4±1.0
	4000	1.066±0.019	24.77±0.61	73.6±2.7	19.4±0.8
AMBTI	6000	1.076±0.014	24.98±0.26	73.4±2.9	19.7±0.8

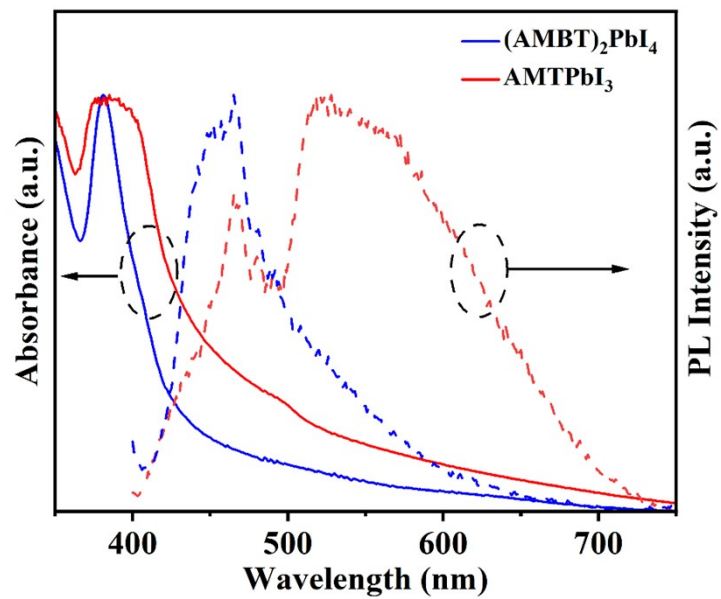


Figure S13. AMTPbI_3 and $(\text{AMBT})_2\text{PbI}_4$ absorption and fluorescence spectra.



Figure S14. pH values of 0.01 M AMTI and AMBTI aqueous solutions.

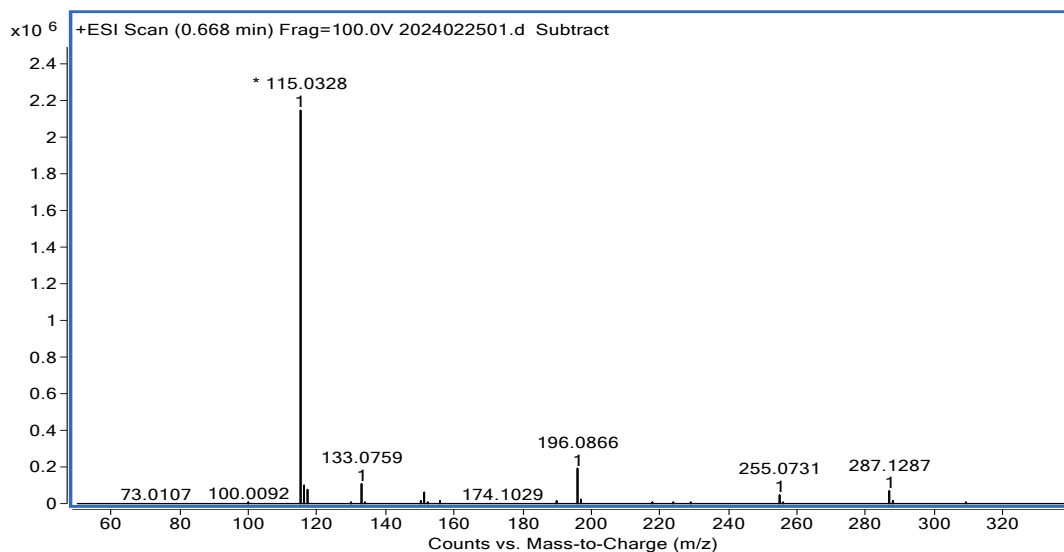


Figure S15a. High-resolution mass spectrum of AMT⁺ (115.0328).

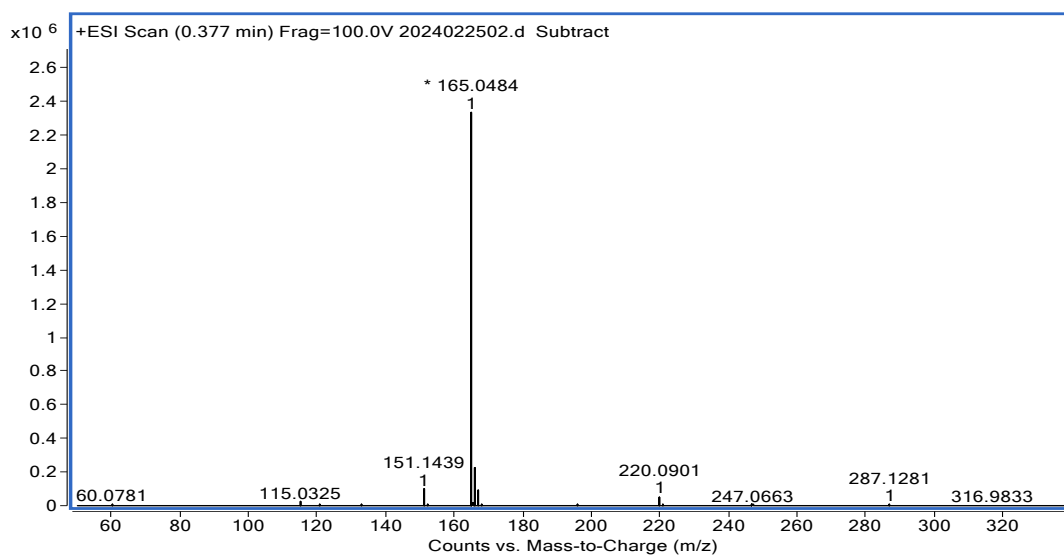


Figure S15b. High-resolution mass spectrum of AMBT⁺ (165.0484).

References

- (1) Kim, M.; Jeong, J.; Lu, H.; Lee, T. K.; Eickemeyer, F. T.; Liu, Y.; Choi, I. W.; Choi, S. J.; Jo, Y.; Kim, H.-B. et al. Conformal quantum dot-SnO₂ layers as electron transporters for efficient perovskite solar cells. *Science* **2022**, 375 (6578), 302.